

Rotational Barriers in Trimethylenemethane–Fe(CO)₂L Complexes. A Density Functional Study

Vicenç Branchadell,[†] Liqun Deng, and Tom Ziegler*

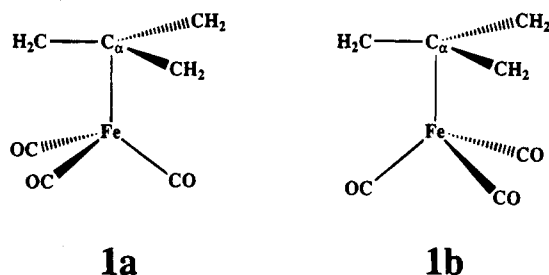
Department of Chemistry, University of Calgary, Calgary, Alberta, Canada T2N 1N4

Received March 8, 1994[⊗]

Density functional calculations have been carried out on the staggered (**1a**) and eclipsed (**1b**) conformations of $\{\eta^4\text{-C}(\text{CH}_2)_3\}\text{Fe}(\text{CO})_2\text{L}$ with L = CO, PF₃, and PH₃. The calculations provide fully optimized structures for **1a** and **1b**. Barriers of rotation, ΔE^b , for the trimethylenemethane ligand around the Fe–C 3-fold axis connecting the staggered equilibrium structures **1a** were calculated to be 78 kJ/mol (L = CO), 81 kJ/mol (L = PH₃), and 79 kJ/mol (L = PF₃), where **1b** represents the transition state for the rotation process. The present calculations indicate that ΔE^b is nearly the same for CO and phosphines. A decomposition of ΔE^b into steric and electronic factors revealed that steric factors contribute to the barrier whereas electronic factors reduce ΔE^b .

I. Introduction

The fluxional motion of ligands coordinated to transition metal fragments has been the subject of many theoretical experimental studies. Trimethylenemethane (TMM) bound to iron tricarbonyl in $\{\eta^4\text{-C}(\text{CH}_2)_3\}\text{Fe}(\text{CO})_3$ is a good example of a ligand with this type of interesting kinetic behavior. The TMM–Fe(CO)₃ complex has a ground state structure¹ in which Fe(CO)₃ and C(CH₂)₃ are arranged in staggered conformation, **1a**. However,



the two trigonal fragments can rotate relative to each other around the 3-fold Fe–C_α symmetry axis connecting the three symmetry equivalent staggered structures, **1a**, with the corresponding eclipsed conformations, **1b**, representing the transition states along the rotational path.

The bonding in **1a** has been the subject of an elegant study due to Albright² et al. It was pointed out in this investigation that the staggered structure, **1a**, is preferred compared to the eclipsed, **1b**, conformation on steric as well as electronic grounds. Albright et al. predicted in addition that the substitution of a CO ligand by a poorer π -acceptor such as PR₃ would enhance the preference of the staggered geometry over the eclipsed conformation by as much as 40 kJ/mol, and thus increase the barrier for the rotation of the C(CH₂)₃ ligand around the Fe–C_α axis in TMM–Fe(PR₃)₃ complexes.

Little is known quantitatively from experiments about the rotational barrier in $\{\eta^4\text{-C}(\text{CH}_2)_3\}\text{Fe}(\text{CO})_3$ due to its high symmetry. However, variable-temperature NMR spectroscopy can be used to determine rotational barriers in species where the symmetry has been lowered by modifying the TMM ligand itself, or by replacing a carbonyl group on iron by a different ligand. For complexes in which the TMM ligand has been modified, $\{\eta^4\text{-RCHC}(\text{CH}_2)_2\}\text{Fe}(\text{CO})_3$ with R = COMe, CHOHe, CHMeOAc, and Et, the free energy of activation, ΔG^\ddagger , for the rotation process was found to be in the narrow range³ between 70 and 75 kJ/mol. Girard et al.⁴ have on the other hand estimated ΔG^\ddagger for a number of CO substituted species, TMM–Fe(CO)₂PR₃ (PR₃ = tertiary phosphine). They find values in the range between 62 and 70 kJ/mol. Thus experiment does not support the theoretical prediction according to which the substitution of CO by tertiary phosphines should lower the rotation barrier. However, it might be argued that the rotation barrier in the tricarbonyl species, $\{\eta^4\text{-RCHC}(\text{CH}_2)_2\}\text{Fe}(\text{CO})_3$, is influenced (increased) by the substitution on the TMM ligand, which makes a direct comparison to the TMM–Fe(CO)₂L difficult.

We shall here present density functional calculations on TMM–Fe(CO)₂L with L = CO, PF₃, and PH₃. Our first objective has been to determine the rotation barrier in TMM–Fe(CO)₃ since it is unattainable by experimental techniques. We shall next calculate the barriers in TMM–Fe(CO)₂L for the phosphine L = PF₃ with a π -acidity comparable to CO as well as the phosphine L = PH₃ considered to be a weak π -acceptor. The present set of calculations should afford a more direct assessment of how the rotational barrier in TMM–Fe(CO)₂L is influenced by L than the one possible by experimental techniques.

II. Computational Details

The reported calculations were carried out by utilizing the program system A-MOL, developed by Baerends et

[†] Permanent address: Departament de Química, Universitat Autònoma de Barcelona, 08193 Bellaterra, Spain.

[⊗] Abstract published in *Advance ACS Abstracts*, June 15, 1994.

(1) Emmerson, G. F.; Ehrlich, K.; Giering, W. P.; Lauterbur, P. C. *J. Am. Chem. Soc.* **1966**, *88*, 3172.

(2) Albright, T. A.; Hoffmann, P.; Hoffmann, R. *J. Am. Chem. Soc.* **1977**, *99*, 7546.

(3) Magyar, E. S.; Lillya, C. P. *J. Organomet. Chem.* **1976**, *116*, 99.

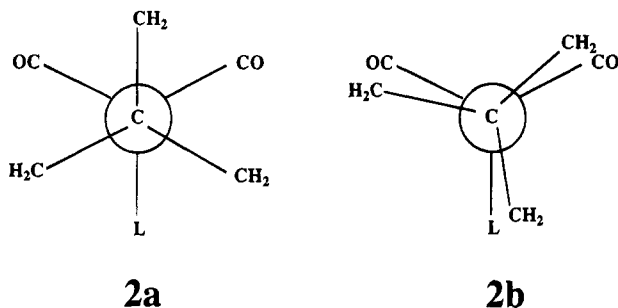
(4) (a) Girard, L.; MacNeill, J. H.; Mansour, A.; Chiverton, A. C.; Page, J. A.; Fortier, S.; Baird, M. C. *Organometallics* **1991**, *10*, 3114.

(b) Girard, L.; Baird, M. C. *J. Organomet. Chem.* **1993**, *444*, 143.

al.^{5,6} and vectorized by Ravenek.^{5b} The numerical procedure applied for the calculations was developed by Boerrigter et al.⁷ The geometry optimization procedure was based on the method developed by Versluis and Ziegler.⁸ The electronic configurations of the molecular systems were described by an uncontracted triple- ζ STO basis set on iron, as well as a double- ζ basis set on carbon, oxygen, phosphorus, fluorine, and hydrogen.⁹ Carbon, oxygen, phosphorus, and hydrogen were given an extra polarization function: $3d_C$ ($\zeta_{3d} = 2.50$), $3d_O$ ($\zeta_{3d} = 2.00$), $3d_P$ ($\zeta_{3d} = 1.4$), and $2p_H$ ($\zeta_{2p} = 1.0$). For fluorine two sets of polarization functions have been used: $3d_F$ ($\zeta_{3d} = 2.0$ and $\zeta_{3d'} = 1.2$). The $1s^2 2s^2 2p^6$ configuration of iron and phosphorus and the $1s^2$ configuration of carbon, oxygen, and fluorine were assigned to the core and treated by the frozen-core approximation. A set of auxiliary¹⁰ s, p, d, f, and g STO functions, centered on all nuclei, was used to fit the molecular density and represent Coulomb and exchange potentials accurately in each SCF cycle. The geometry has been optimized within the local density approximation (LDA), using the parametrization of the local exchange-correlation potential due to Vosko et al.¹¹ Becke's¹² nonlocal exchange correction and Perdew's¹³ nonlocal correlation correction have been incorporated as perturbations for the LDA optimized geometries to calculate energy differences.

III. Results and Discussion

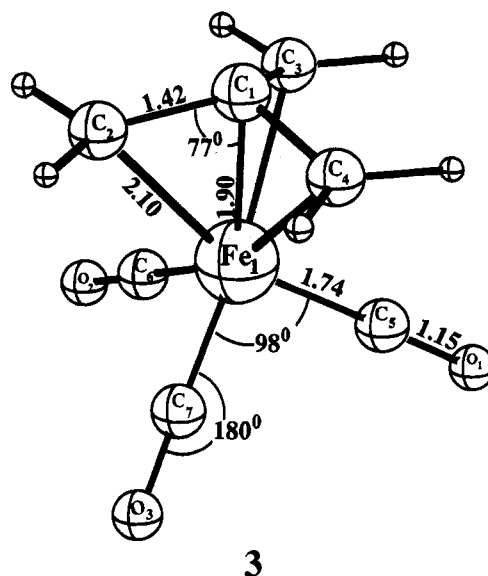
Calculations have been carried out on the rotational barriers of the complexes $TMM-Fe(CO)_2L$: $TMM = \eta^4-(C(CH_2)_3)$; $L = CO, PH_3,$ and PF_3 . We have considered two different conformations for each complex: staggered and eclipsed. The Newman projections of these conformations are represented in **2a** and **2b**. The three



symmetry equivalent staggered conformations, **2a**, correspond to the energy minima, while the eclipsed

conformations, **2b**, correspond to the transition states linking these minima along the rotation path.

The staggered and eclipsed conformations of the $TMM-Fe(CO)_3$ complex have been optimized within C_{3v} constraints as **3** and **4**, respectively. The optimized geometry for $TMM-Fe(CO)_3$ in the staggered conforma-



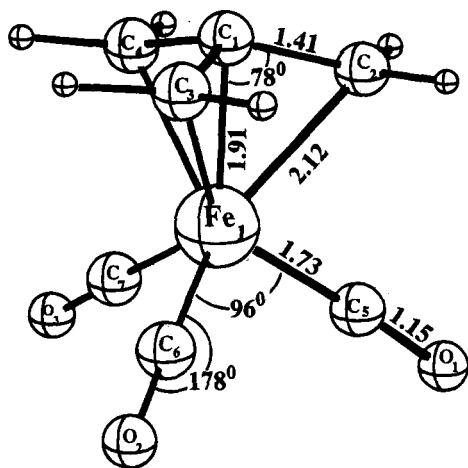
tion, **3**, can be compared to the experimental structure determined by electron diffraction.^{14,15} The calculated deviation of the TMM ligand from planarity with a $Fe-C_1-C_2$ angle of 77° is in excellent agreement with experiment, as is the predicted $CO-Fe-CO$ angle of 98° . The calculated $Fe-C_1$ and $Fe-C_2$ distances involving TMM are respectively 0.04 and 0.02 Å shorter than the experimental values,^{14,15} whereas the calculated $Fe-CO$ bond length is too short by 0.07 Å. It is well-known¹⁶ that the LDA scheme underestimates bond distances by 0.02–0.04 Å, still the deviation in the $Fe-CO$ bond is surprisingly large. The agreement with experiment can be improved by including nonlocal corrections in the geometry optimization step.⁶ However, we do not feel that the much more costly nonlocal optimization calculations are required to meet the objective of the present study.

Compared to **3**, the $Fe-TMM$ distances in the eclipsed structure, **4**, are slightly longer by 0.01–0.02 Å and the deviation of the TMM ligand from planarity is reduced with a $Fe-C_1-C_2$ angle of 78° . The apparent decrease in the $Fe-TMM$ interaction is compensated for by stronger $Fe-CO$ bonds in which the distance has been reduced by 0.01 Å.

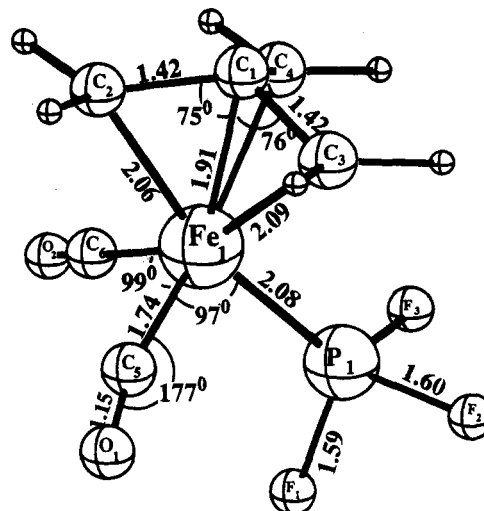
The geometries of the $TMM-Fe(CO)_2(PH_3)$ and $TMM-Fe(CO)_2(PF_3)$ complexes have been optimized within C_s constraints. The optimized structures of the staggered and eclipsed conformations of the $TMM-Fe(CO)_2(PH_3)$ complex are given in **5** and **6**, respectively, and those corresponding to the $TMM-Fe(CO)_2(PF_3)$ complex are given in **7** and **8**, respectively. We note again in the $TMM-Fe(CO)_2L$ systems with $L = PH_3$ and

(5) Baerends, E. J.; Ellis, D. E.; Ros, P. *Chem. Phys.* **1973**, *2*, 41.
 (6) (a) Baerends, E. J. Ph.D. Thesis, Vrije Universiteit, Amsterdam, 1975. (b) Ravenek, W. In *Algorithms and Applications on Vector and Parallel Computers*; te Riele, H. J. J., Dekker, Th. J., van de Vorst, H. A., Eds.; Elsevier: Amsterdam, 1987.
 (7) Boerrigter, P. P.; te Velde, G.; Baerends, E. J. *Int. J. Quantum Chem.* **1988**, *33*, 87.
 (8) Versluis, L.; Ziegler, T. *J. Chem. Phys.* **1988**, *88*, 322.
 (9) (a) Snijders, G. J.; Baerends, E. J.; Vernooijs, P. *At. Nucl. Data Tables* **1982**, *26*, 483. (b) Vernooijs, P.; Snijders, G. J.; Baerends, E. J. *Slater Type Basis Functions for the whole Periodic System*; Internal Report; Free University of Amsterdam: Amsterdam, The Netherlands, 1984.
 (10) Krijn, J.; Baerends, E. J. *Fit Functions in the HFS Method*; Internal report (in Dutch); Free University of Amsterdam: Amsterdam, The Netherlands, 1984.
 (11) Vosko, S. H.; Wilk, L.; Nusair, M. *Can. J. Phys.* **1990**, *58*, 1200.
 (12) Becke, A. D. *Phys. Rev.* **1988**, *A38*, 2398.
 (13) Perdew, J. P. *Phys. Rev.* **1986**, *B33*, 8822; Erratum. *Ibid.* **1986**, *B34*, 7406.

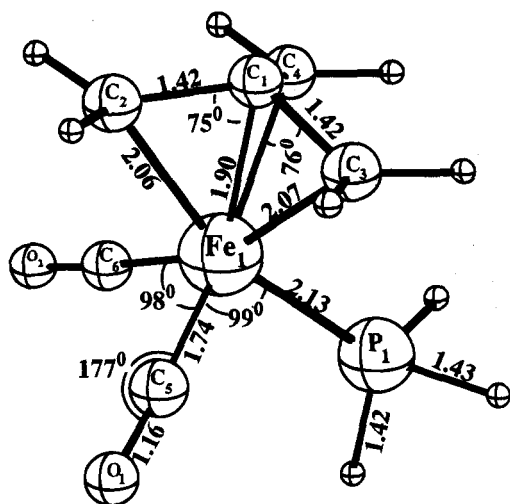
(14) Reference 15: $Fe-C_1 = 1.938$ Å, $Fe-C_2 = 2.133$ Å, $Fe-C_3 = 1.810$ Å, $C-O = 1.153$ Å, $C_7-Fe-C_5 = 99.2^\circ$, $C_2-C_1-Fe = 76.4^\circ$.
 (15) Almenningen, A.; Haaland, A.; Wahl, K. *Acta Chem. Scand.* **1969**, *23*, 1145.
 (16) Fan, L.; Ziegler, T. *J. Chem. Phys.* **1991**, *95*, 7401.



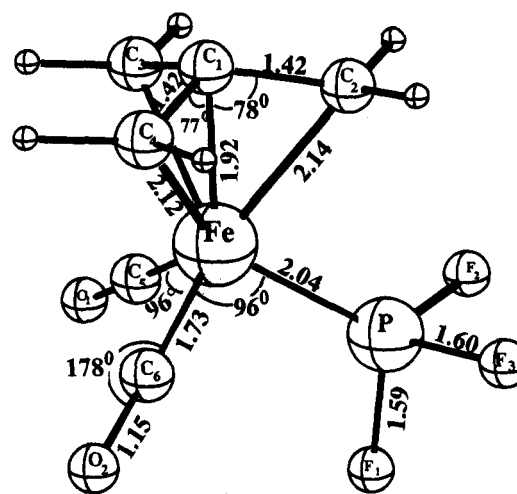
4



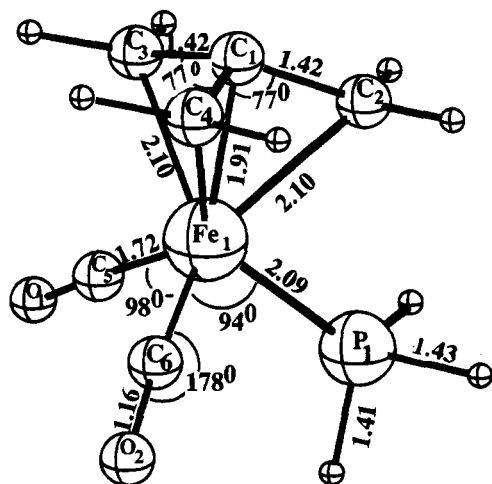
7



5



8



6

PF₃ that the TMM-Fe distances increase from the staggered to the eclipsed conformations whereas the Fe-CO and Fe-P distances follow the reverse trend. The optimized geometry for 5 can be compared with the X-ray diffraction structure of TMM-Fe(CO)₂PCy₂Ph.^{2a,17} The largest deviation is in the Fe-P distance where we find R(Fe-PH₃) = 2.13 Å as opposed to R(Fe-PCy₂Ph) = 2.263 Å in the experimental structure. The deviation

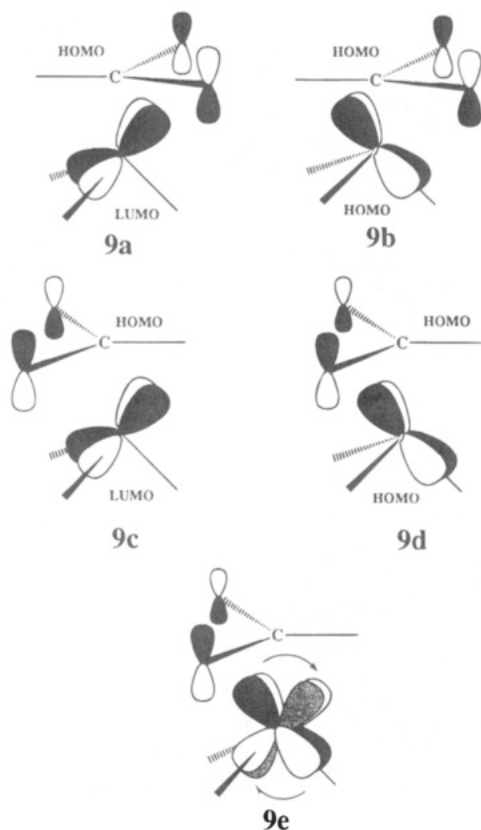
might in part be a result of the larger steric bulk on the PCy₂Ph ligand.

The computed rotational barriers, ΔE^b , for the three complexes are presented in Table 1. These values are very similar for all the complexes, despite the different nature of the ligand L. If we compare the results corresponding to CO and PH₃ with experimental values,^{3,4a} we observe that the computed values are slightly higher. According to our results the substitution of CO by a phosphine does not produce an important increase in the rotational barrier. These results are in closer agreement with experimental observations. Albright² et al. found for TMM-FeL₃ an increase of 40 kJ/mol in going from L = CO to L = PR₃. However, it is not clear how relevant this result is to the TMM-Fe(CO)₂L systems studied here in which only one CO is substituted by a phosphine. Also the results obtained by Albright² et al. were based on a rigid rotation.

Albright² et al. viewed TMM-FeL₃ as a complex between C(CH₂)₃²⁻ and FeL₃²⁺, with the interactions between the two fragments involving the HOMO of C(CH₂)₃²⁻ as well as the HOMO and LUMO of FeL₃²⁺.

(17) Reference 2a: Fe-C1 = 1.934 Å, Fe-C2 = 2.129 Å, Fe-C3 = 2.128-2.138 Å, Fe-C5 = 1.749-1.758 Å, Fe-P = 2.263 Å, C-O = 1.156 Å, C1-C2 = 1.421 Å, C1-C3 = 1.41 Å, C5-Fe-C6 = 98.0°, C5-Fe-P = 95.4-97.5°.

In applying this picture to $\text{TMM-Fe(CO)}_2\text{L}$, one finds in the staggered conformation that the HOMO of $\text{C(CH}_2)_3^{2-}$ can interact with the LUMO of $\text{Fe(CO)}_2\text{L}^{2+}$ in a bonding fashion, **9a**, whereas the repulsive four-



electron two-orbital interaction, **9b**, between the two HOMO's is kept at a minimum due to the vanishing overlap. In the eclipsed conformation, **2b**, the two HOMO's overlap, **9d**, resulting in a destabilizing steric interaction. Further the HOMO–LUMO interaction, **9c**, in the eclipsed conformation is not as favorable due to the tilt of the d orbital on the metal.

We have decomposed the calculated rotation barrier, ΔE^b , into components that are related to the above analysis by Albright et al. The decomposition is based on the extended transition state method¹⁸ (ETS) and allows us to write the energy barrier as

$$\Delta E^b = \Delta E_{\text{st}}^b + \Delta E_{\text{el}}^b + \Delta E_{\text{prep}}^b \quad (1)$$

Here the first term to the right represents the contribution to the barrier from the four-electron two-orbital steric interactions, including **9a** and **9c**, whereas the second term takes into account the contributions from the two-orbital two-electron interactions, such as **9b** and **9d**. The last term stems from the change in the geometry of the two fragments. It should be pointed out that the first term also includes a small contribution from the difference between the electrostatic interactions of the two fragments in the staggered and eclipsed conformations.

The results from the decomposition are shown in Table 1. It is clear that the steric term ΔE_{st}^b strongly

Table 1. Calculated Barriers^a of Rotation for $\text{TMM-Fe(CO)}_2\text{L}$

L	ΔE^b	ΔE_{st}^b	ΔE_{el}^b	ΔE_{prep}^b
CO	78	142	-62	-2
PH ₃	81	131	-58	-12
PF ₃	79	128	-60	-11

^a All energies in kJ/mol.

favors **2a** over **2b**. This is in part due to the smaller repulsion in **9a** compared to **9c**. The steric contribution of 143 kJ/mol for L = CO is only slightly larger than the same contribution in the two phosphines with $\Delta E_{\text{st}}^b = 131$ kJ/mol for L = PH₃ and 128 kJ/mol for L = PF₃.

The electronic term is seen to reduce the rotation barrier, thus ΔE_{el}^b favors **2b** over **2a**, and it is the same for all three ligands, Table 1. One might have expected that ΔE_{el}^b would prefer **2a** over **2b**, and thus add to the barrier, since **9b** is more favorable than **9d**. In the first place, the HOMO–LUMO overlaps¹⁹ of 0.27 and 0.24 for **9a** and **9c**, respectively, in the case of L = CO are not vastly different. Further, the HOMO–LUMO interactions displayed in **9a** and **9c** are not the only contributions to ΔE_{el}^b . The additional contributions represent charge polarizations within each fragment aimed at alleviating the steric repulsions. The polarizations are particularly important in **2b** with the strong repulsive interaction **9d**, and the main polarization in the eclipsed conformation is due to a shift of charge from the HOMO to the LUMO of Fe(CO)_3 , **9e**. This transfer²⁰ is virtually absent in **1a** where the occupation of the HOMO on Fe(CO)_3 is 1.98 e (L = CO), but constitute 0.18 e in **1b** where the corresponding population is 1.82 e. It is the charge transfer, **9e**, which represents the major contribution to ΔE_{el}^b . There is also a minor contribution from the rearrangement of the fragments, ΔE_{prep}^b . This contribution comes primarily from the Fe–CO and Fe–P bond contractions in the eclipsed structure, **6** and **8**.

IV. Concluding Remarks

We have carried out density functional calculations on the rotation barrier in $\{\eta^4\text{-C(CH}_2)_3\}\text{Fe(CO)}_2\text{L}$ with L = CO, PF₃, and PH₃. It was found that the barrier is insensitive to the nature of the ligand L. This finding is in agreement with experimental observations. An energy decomposition analysis based on the ETS scheme¹⁸ revealed that steric factors contribute strongly to the barrier, whereas electronic contributions reduce the barrier. Fully optimized structures have been provided for the staggered and eclipsed conformations.

Acknowledgment. This investigation was supported by the Natural Sciences and Engineering Re-

(18) (a) Ziegler, T.; Rauk, A. *Theor. Chim. Acta* **1977**, *46*, 1. (b) Ziegler, T.; Rauk, A. *Inorg. Chem.* **1979**, *18*, 1558.

(19) These are the overlaps for L = CO. Similar small differences were calculated for L = PH₃ and PF₃.

(20) The transfer of charge from the HOMO to the LUMO of the metal fragment $\text{Fe(CO)}_2\text{L}$ was also calculated to be ~ 0.2 e for L = PH₃ and L = PF₃ in the eclipsed conformation of $\text{TMM-Fe(CO)}_2\text{L}$.

search Council of Canada (NSERC). The University of Calgary is acknowledged for access to the IBM-6000/RISC facilities. This work was supported in part by the donors of the Petroleum Research Fund, administered by the American Chemical Society (ACS-PRF No. 27023-AC3). V.B. gratefully acknowledges financial

support from the Comissió Interdepartamental de Recerca i Innovació Tecnològica (CIRIT) of the Catalonia government. We would like to thank professor M. C. Baird (Queens University) for many valuable discussions.

OM9401770